The Astrophysical Journal Letters, 831:L17 (6pp), 2016 November 10 doi:10.3847/2041-8205/831/2/L17

EVIDENCE OF AGB POLLUTION IN GALACTIC GLOBULAR CLUSTERS FROM THE Mg–Al ANTICORRELATIONS OBSERVED BY THE APOGEE SURVEY

P. Ventura[1], D. A. García-Hernández[2,3], F. Dell'Agli[1], F. D'Antona[1], Sz. Mészáros[4], S. Lucatello[5], M. Di Criscienzo[1], M. Shetrone[6], M. Tailo[1], Baitian Tang[7], and O. Zamora[2,3]
[1] INAF–Osservatorio Astronomico di Roma, via Frascati 33, I-00077 Monteporzio, Italy
[2] Instituto de Astrofísica de Canarias (IAC), E-38205 La Laguna, Tenerife, Spain
[3] Departamento de Astrofísica, Universidad de La Laguna (ULL), E-38206 La Laguna, Spain
[4] ELTE Gothard Astrophysical Observatory, H-9704 Szombat-hely, Szent Imre Herceg st. 112, Hungary
[5] INAF–Osservatorio Astronomico di Padova, vicolo dell'Osservatorio 5, I-35122 Padova, Italy
[6] University of Texas at Austin, McDonald Observatory, Austin, TX, USA
[7] Departamento de Astronomía, Casilla, 160-C, Universidad de Concepción, Concepción, Chile
Received 2016 September 26; revised 2016 October 10; accepted 2016 October 10; published 2016 November 4

ABSTRACT

We study the formation of multiple populations in globular clusters (GCs), under the hypothesis that stars in the second generation formed from the winds of intermediate-mass stars, ejected during the asymptotic giant branch (AGB) phase, possibly diluted with pristine gas, sharing the same chemical composition of first-generation stars. To this aim, we use the recent Apache Point Observatory Galactic Evolution Experiment (APOGEE) data, which provide the surface chemistry of a large sample of giant stars, belonging to clusters that span a wide metallicity range. The APOGEE data set is particularly suitable to discriminate among the various pollution scenarios proposed so far, as it provides the surface abundances of Mg and Al, the two elements involved in a nuclear channel extremely sensitive to the temperature, hence to the metallicity of the polluters. The present analysis shows a remarkable agreement between the observations and the theoretical yields from massive AGB stars. In particular, the observed extension of the depletion of Mg and O and the increase in Al is well reproduced by the models and the trend with the metallicity is also fully accounted for. This study further supports the idea that AGB stars were the key players in the pollution of the intra-cluster medium, from which additional generations of stars formed in GCs.

Key words: globular clusters: general – stars: abundances – stars: AGB and post-AGB

1. INTRODUCTION

The spectroscopic and photometric astronomical data accumulated in the past decades have discredited the classic paradigm that globular cluster (GC) stars represent a simple stellar population. Results from high-resolution spectroscopy outlined star-to-star differences in the abundances of the light elements, suggesting the signature of proton-capture nucleosynthesis (Gratton et al. 2012). The discovery of multiple main sequences (MS) in the color–magnitude diagrams of some GCs (Piotto et al. 2007) indicated the existence of a group of stars enriched in He, thus further confirming the hypothesis that part of the stars in GC formed from proton-capture contaminated matter.

Several self-enrichment mechanisms have been proposed so far to explain the formation of multiple populations in GC: the asymptotic giant branch (AGB) scenario (Ventura et al. 2001; D'Ercole et al. 2008), fast rotating massive stars (Decressin et al. 2007), interacting massive binaries (de Mink et al. 2009), core H-burning in supermassive MS stars (Denissenkov & Hartwick 2014), and the accretion model (Bastian et al. 2013). The difficulties encountered by the different scenarios in accounting for the various observational evidences have been recently discussed in Renzini et al. (2015).

Until now, the theoretical attempts to reproduce the abundance patterns observed in GC stars have been mainly focused on the O–Na anticorrelation (as obtained from high-resolution optical spectroscopy), which has been detected in essentially all Galactic GC where the compositions for more than a handful of stars have been measured (see, e.g., Carretta et al. 2009). High-resolution near-IR massive spectroscopic surveys like the Apache Point Observatory Galactic Evolution Experiment (APOGEE; Majewski et al. 2016) are going to strongly augment these previous optical studies. This is because APOGEE provides: (i) the chemical abundances of key elements like Fe, Mg, Al, etc., from neutral H-band lines that are expected to be less affected by nonlocal thermodynamic equilibrium effects than those in the optical range (see, e.g., García-Hernández et al. 2015); and (ii) a higher number of GC stars (compared to literature) analyzed in a homogeneous way, and covering GC of various mass and metallicity (Mészáros et al. 2015). Indeed, the Mg–Al distributions are much clearer in the APOGEE data (Mészáros et al. 2015) than in previous optical studies (e.g., Carretta et al. 2013).

The analysis of the Mg–Al anticorrelation offers a better opportunity to deduce the nature of the polluters in comparison to the traditional O–Na trend, for the following reasons: (a) the activation of the Mg–Al nucleosynthesis requires higher temperatures than the CNO and NeNa cycles, thus allowing us to further restrict the range of temperatures at which the contaminated matter was exposed; (b) the Mg and Al abundances of red giant branch (RGB) stars definitively reflect the initial chemical composition, as no change in the surface abundance of these elements occurs during the RGB phase; unlike O and Na, whose surface content can be affected by deep mixing (Denisenkov & Denisenkova 1990).

Here, we interpret the recent APOGEE data of GC stars (Mészáros et al. 2015), which clearly show that the matter from which second-generation (SG) stars formed was depleted in

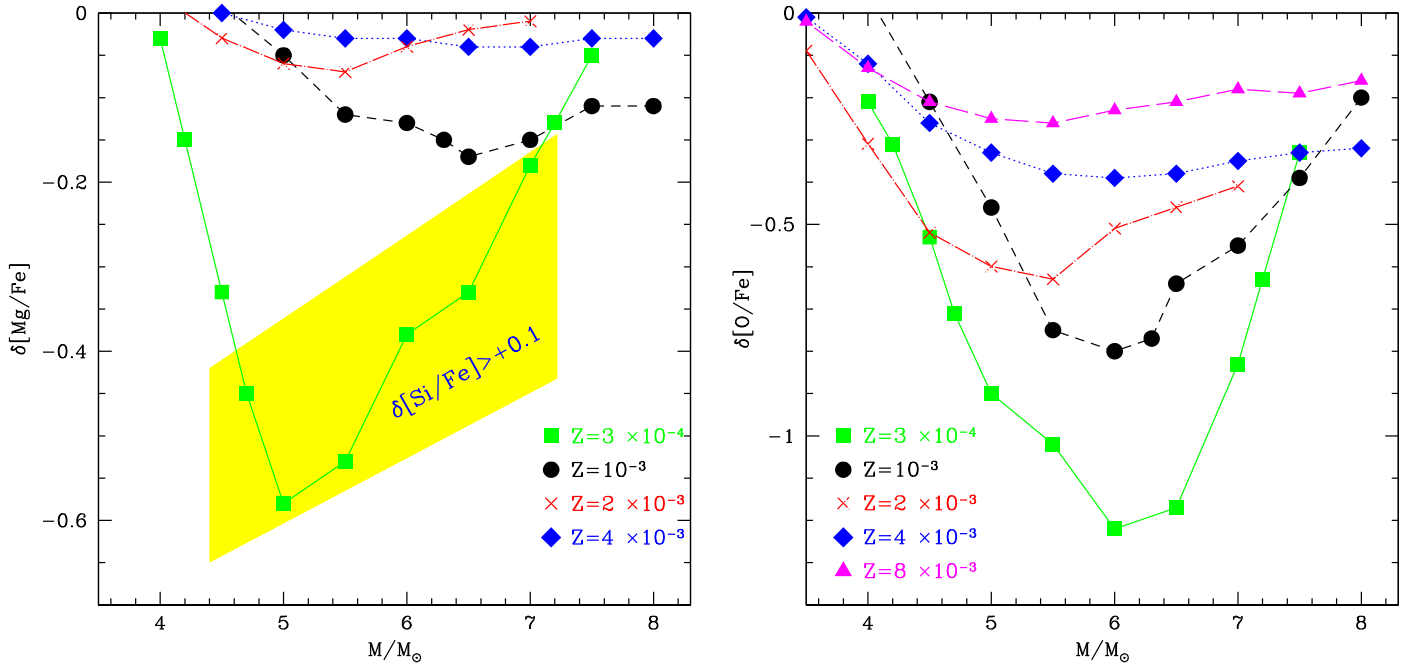

Figure 1. Average depletion of Mg (left) and O (right) in models of different mass and metallicity. The meaning of the symbols is as follows: green squares, black points, and magenta triangles indicate, respectively, $Z = 3 \times 10^{-4}$, $Z = 10^{-3}$, and $Z = 8 \times 10^{-3}$ models by Ventura et al. (2013); blue diamonds and red crosses correspond, respectively, to $Z = 4 \times 10^{-3}$ models by Ventura et al. (2014) and to unpublished, $Z = 2 \times 10^{-3}$ models. The yellow, shaded area in the left panel includes the models that produce a Si enrichment above 0.1 dex. The $Z = 8 \times 10^{-3}$ models are not shown in the left panel, as no significant Mg depletion occurs.

Mg. This finding rules out fast rotating massive stars and massive binaries as possible polluters, as well as the accretion scenario hypothesis.[8] We concentrate on the AGB scenario, in which SG stars in GC formed from the winds of massive AGB stars (AGBs), mixed with pristine gas in the cluster. We base our analysis on five GCs, selected to span a wide range of metallicities and with a number of stars observed sufficiently large enough to allow a statistical interpretation of the results obtained.

To date, this is the first investigation where the AGB scenario is tested against an extensive data set of Mg and Al abundances. This study is the most severe and reliable test of the role that AGB stars may have played in the self-enrichment of GC, as it allows us to fix with an unprecedented accuracy the extent of the nucleosynthesis to which the contaminating matter was exposed and, more importantly, how this changes with metallicity.

2. POLLUTION FROM MASSIVE AGB STARS

Pollution from stars of mass above $\sim 3\,M_{\odot}$ is determined by hot bottom burning, the nuclear activity taking place at the base of the convective envelope (CE) during each interpulse (Blöcker & Schönberner 1991). The temperature at the bottom of the CE, $T_{\rm bce}$, is the key quantity in determining the degree of the nucleosynthesis experienced and the chemical composition of the gas ejected into the interstellar medium. The activation of CN cycling takes place when $T_{\rm bce} \sim 40$ MK, whereas O burning and Na production (via ^{22}Ne proton capture) require $T_{\rm bce} \sim 80$ MK; at $T_{\rm bce} \sim 100$ MK, Mg is efficiently destroyed by proton fusion, starting a series of reactions leading to the synthesis of Al. At even higher $T_{\rm bce}$, part of the synthesized Al produces Si, via proton capture.

The nucleosynthesis activated at the base of the CE is extremely sensitive to the mass and the metallicity: (a) stars of higher mass evolve on more massive cores, thus reaching higher temperatures and experiencing a more advanced nucleosynthesis; (b) lower-metallicity stars evolve at larger $T_{\rm bce}$, thus they experience a more efficient proton-capture burning.

The depletion of Mg and O in the gas lost by AGB stars in models of various mass and metallicity is shown in Figure 1. These results refer to $Z = 3 \times 10^{-4}$, $Z = 10^{-3}$ and $Z = 8 \times 10^{-3}$ models by Ventura et al. (2013), to $Z = 4 \times 10^{-3}$ models by Ventura et al. (2014), and to unpublished models of metallicity $Z = 2 \times 10^{-3}$. In all cases, mass loss was modeled according to Bloecker (1995), where $\dot{M} \sim L^{4.2}/T_{\rm eff}^2$, with no explicit dependency on the surface chemistry.

Basically, we find the following: (a) CN cycling is activated in the whole range of mass and metallicity explored here; (b) O destruction occurs in stars of mass above $\sim 4\,M_{\odot}$, with efficiency decreasing with increasing Z; (c) Na is synthesized via ^{22}Ne-burning in the same range of masses at which O destruction takes place; (d) Mg depletion occurs only in low-metallicity massive AGB stars; (e) Si is produced only in $Z < 5 \times 10^{-4}$ massive AGBs.

Figure 1 shows that Mg depletion, compared to O burning, is achieved only in low-metallicity AGBs. Furthermore, the synthesis of Al is extremely sensitive to metallicity, at odds with Na production, which, for the reasons given above, is effective in all the AGB models of mass above $\sim 4\,M_{\odot}$, independently of Z. It is for these reasons that the investigation of the Mg–Al anticorrelation is a much more efficient tool, compared to the classic O–Na trend, to explore and test all the predictions of the AGB scenario for the formation of multiple populations in GC.

[8] We do not discuss the supermassive MS stars hypothesis because no self-consistent model based on hydrodynamic simulations has been presented so far and it is not yet clear if and how the nucleosynthesis associated with this mechanism is sensitive to metallicity.

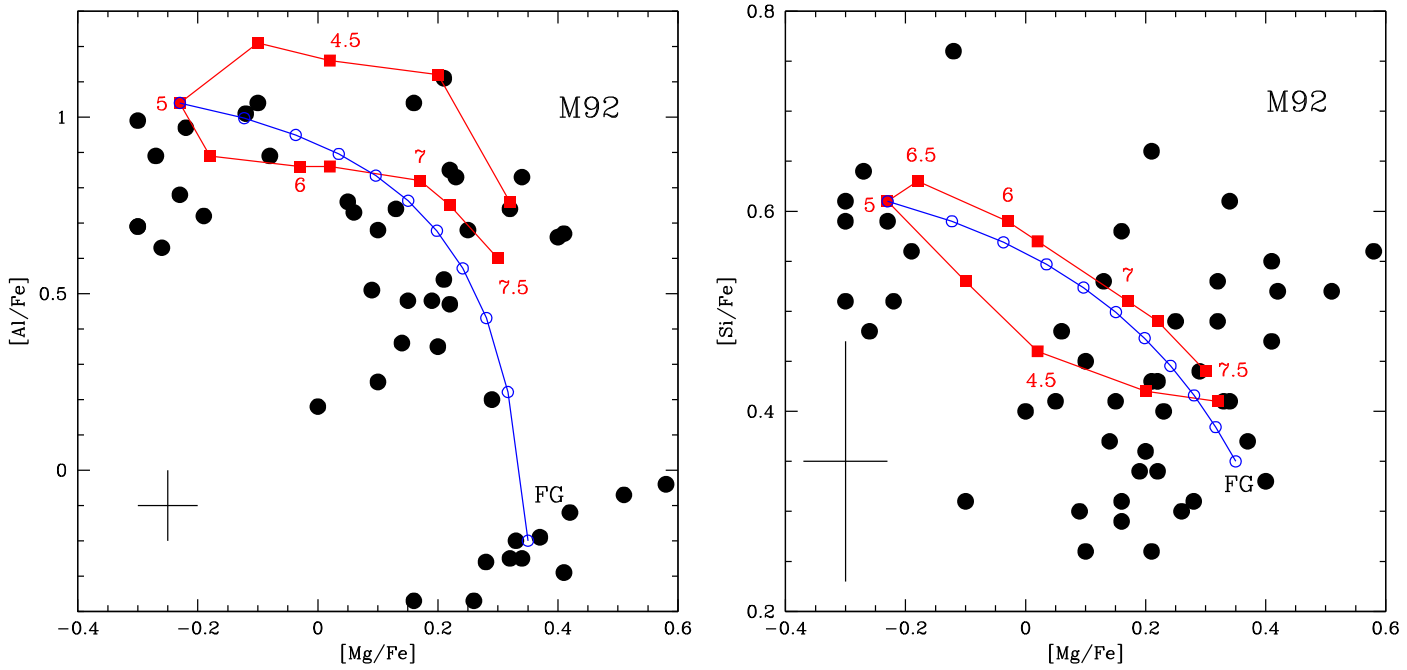

Figure 2. M92 stars from Mészáros et al. (2015) are shown as full dots in the Mg–Al (left) and Mg–Si (right) planes. The black crosses indicate typical error bars. The yields of AGB models of metallicity $Z = 3 \times 10^{-4}$ are indicated with red squares; the numbers close to the squares indicate the initial masses. Blue, open circles indicate the chemistry expected from mixing of the AGB ejecta with pristine gas, with percentages of the latter ranging from 0% to 100%, in steps of 10%. The points corresponding to 100% dilution are close to the FG label.

Table 1
The Chemical Properties of Globular Clusters

GC ID	GC Name	[Fe/H]	Δ [Si/ Fe]	Δ [Al/ Fe]	Δ [Mg/ Fe]	Δ [O/ Fe]
NGC 6341	M92	−2.23	0.06	0.93	0.28	0.27
NGC 6205	M13	−1.50	0.02	0.95	0.12	0.36
NGC 5272	M3	−1.40	0.01	0.87	0.08	0.23
NGC 5904	M5	−1.24	…	0.70	0.03	0.25
NGC 6171	M107	−1.01	…	0.02	…	0.09

Note. The entries in columns 4–7 give the spread between the average mass fractions of Si, Al, Mg, and O in stars belonging to the FG and SG of the cluster, as identified by Mészáros et al. (2015).

3. UNDERSTANDING THE CHEMICAL PATTERNS OF GC STARS

In the interpretation of the APOGEE data, we focus on M92, M3, M13, M5, and M107. This choice is motivated by the wide spread in metallicity spanned by the stars in these clusters and, for the most metal-poor GC, by the large number of giants observed. This allows, at least on qualitative grounds, an approach aimed at understanding how star formation occurred in these stellar systems. Although the APOGEE data include C and N, here we focus on Mg, Si, Al, and O because: (a) CN cycling is much less sensitive to metallicity compared to the nuclear channels involving the heavier species; (b) C and N are subject to possible alterations during the RGB evolution, which prevents a straightforward interpretation of the measured abundances. The data of the clusters used in the present analysis are reported in Table 1. We discuss the individual clusters separately, starting with the most metal-poor GC M92 and ending with the most metal-rich M107.

3.1. M92

M92 is the lowest-metallicity GC in our sample. Figure 2 shows the observed Mg–Al and Mg–Si trends; the observations are compared with the $Z = 3 \times 10^{-4}$ models shown in Figure 1. On the same planes we also show a dilution curve, obtained by mixing different fractions of the AGB ejecta with pristine gas. To have an idea of the largest degree of contamination expected, here and in the following the dilution patterns are based on the chemistry of the AGB models showing the largest modification with respect to the initial chemistry; Ventura & D'Antona (2011) showed that this is found for the stars whose mass is just below the threshold required to activate C-burning and develop a core composed of O and Ne.

The chemical composition of AGBs nicely reproduces the observations, particularly the spread in Mg (0.6 dex), Al (1 dex), and Si (0.2 dex). These results confirm that the contaminated matter was exposed to a very advanced nucleosynthesis, above ∼100 MK, in agreement with the predictions of low-metallicity AGB models.

According to our interpretation, the stars with the most contaminated chemical composition, in the upper left regions of the panels of Figure 2, formed from the ashes of the evolution of massive AGBs, with little dilution with pristine gas.

The sample of M92 giants shown in Figure 2 is completed by first-generation (FG) stars, sharing the same chemical composition of the pristine gas, and an additional group of giants, whose chemistry invokes dilution of the AGB winds with 30%–70% of pristine gas. This suggests that the formation of SG stars in M92 took place as a rather continuous process, though possible gaps in the formation of the SG cannot be ruled out based on the present data.

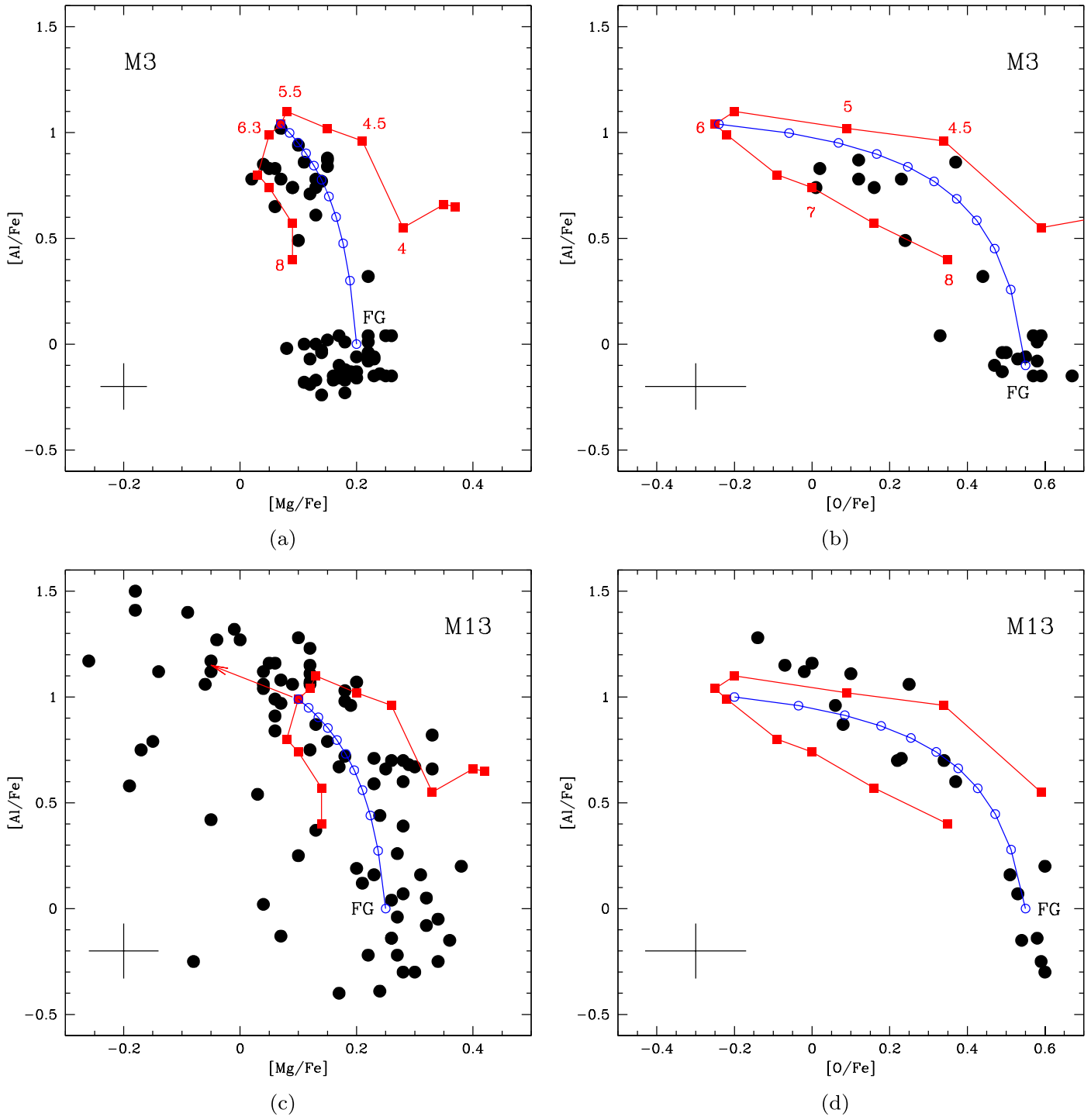

Figure 3. Mg–Al (left) and O–Al (right) trends defined by stars in M3 (top) and M13 (bottom). The observations are compared with AGB models of metallicity $Z = 10^{-3}$. The meaning of the symbols is the same as in Figure 2.

3.2. M3 and M13

The Mg–Al and O–Al trends traced by M3 and M13 stars are shown in Figure 3, where they are compared with the ejecta of $Z = 10^{-3}$ AGBs.

The models reproduce the position on the Mg–Al and O–Al planes of the M3 stars with the most contaminated chemical composition. Compared to M92, a narrower Mg distribution is found here, consistently with the higher metallicity of M3 and with the results shown in Figure 1. The largest O-depletion observed is ∼0.2–0.3 dex lower than the AGB yields, suggesting that dilution with pristine gas occurred in the formation of the SG; conversely, the observed Mg depletion of the same group of objects is well reproduced by the models. These results might suggest that the predicted Mg depletion is slightly underestimated at these metallicities.

The lower right panel of Figure 3 shows that the observed O–Al trend of M13 is nicely reproduced: the M13 stars with most extreme chemical composition show O-depletion

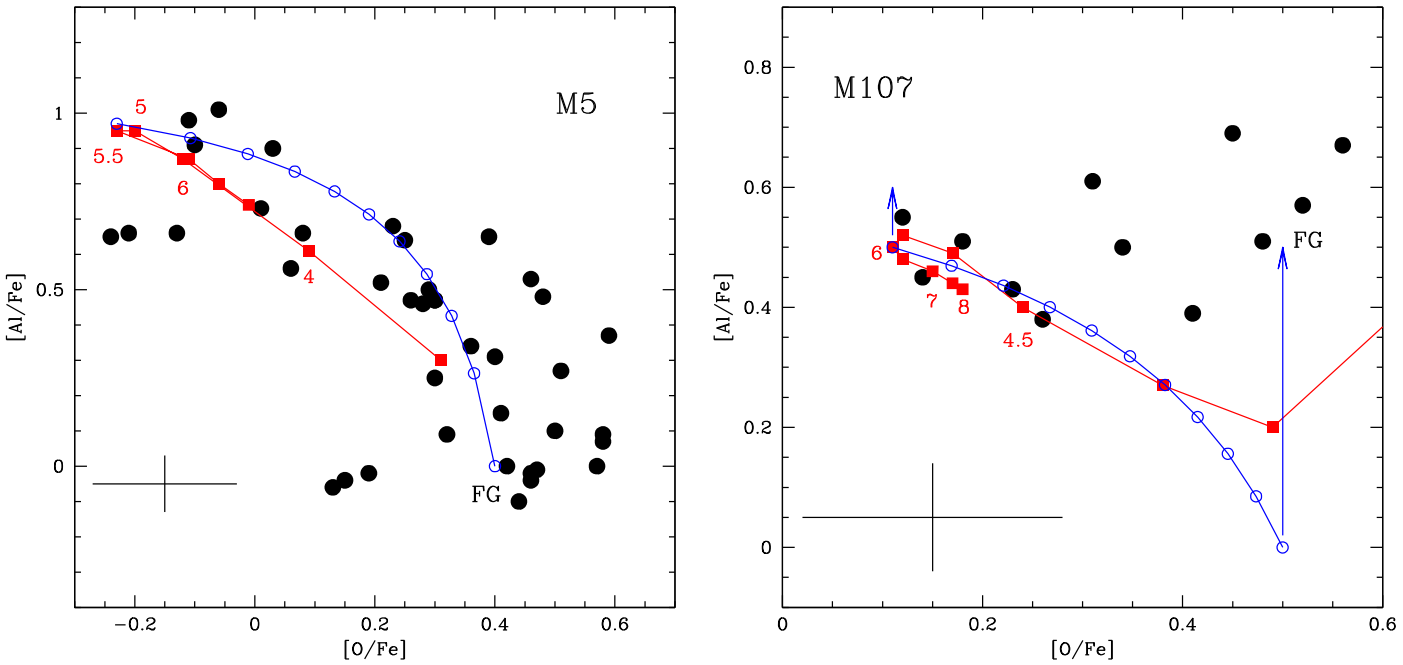

Figure 4. O–Al trends defined by stars in M5 (left) and M107 (right), compared with AGB models of metallicity, respectively, $Z = 2 \times 10^{-3}$ and $Z = 4 \times 10^{-3}$. The arrows on the right indicate the change in the dilution curve when the higher Al of FG stars in M107 is considered.

(δ[O/Fe] $= -0.6$) and Al-enhancement (δ[Al/Fe] ~ 1) in agreement with the theoretical predictions.

In the Mg–Al plane, a few stars show a Mg depletion (∼0.2 dex) in excess of the theoretical expectations, once more suggesting the need for a slightly higher Mg depletion. This problem was addressed by D'Antona et al. (2016) and Ventura et al. (2011), who discussed the possibility that a factor of ∼2 increase in the cross-section of the ^{25}Mg(p,γ)^{26}Al reaction was required to fill this gap. The expected results, indicated with an arrow in the bottom left panel of Figure 3, confirm that the agreement with the data would be significantly improved. We leave this problem open.

In the relative comparison between the two clusters, the distributions of stars in the various planes indicate that, on average, the SG of M13 is more contaminated by the AGBs ejecta, whereas in the case of M3 a higher degree of dilution with pristine gas occurred.

3.3. M5

The Mg–Al trend defined by M5 stars is rather peculiar, as there is no appreciable Mg spread (δ[Mg/Fe] < 0.03), while the Al-spread is about a factor of 10 (Mészáros et al. 2015). This can be understood based on the behavior of the $Z = 2 \times 10^{-3}$ lines in Figure 1. Indeed, the M5 metallicity is just above the threshold required to achieve a significant Mg depletion, but is still sufficiently low that Al-synthesis occurs (this apparently anomalous behavior is due to the large difference in the initial mass fractions of the two elements, such that the consumption of a small percentage of Mg is sufficient to allow a significant Al production).

The results in the O–Al plane (left panel of Figure 4) show that the chemistry of the AGB ejecta nicely compares with the chemical composition of the SG stars: the largest O-depletion (δ[O/Fe] $= -0.5$) and Al-increase (δ[Al/Fe] $= 1$) are nicely reproduced by the AGB models. The difference between the O spread defined by M5 (δ[O/Fe] $= -0.5$) and M13 (δ[O/Fe] $= -0.7$) stars is in agreement with the results from AGB models of the metallicity of the two clusters, as can be deduced from the comparison between the $Z = 10^{-3}$ and $Z = 2 \times 10^{-3}$ lines in Figure 1.

The observations apparently trace a continuous trend, suggesting that SG stars in M5 formed from the gas ejected from massive AGBs diluted at various extents with pristine matter.

3.4. M107

M107 is the most metal-rich cluster examined here. Although the number of stars with available O abundances (Mészáros et al. 2015) is not as large as in the other clusters, we prefer to discuss it because this allows a wider exploration of the metallicity effects.

No Mg spread is detected, a consequence of the poor efficiency of Mg-burning in AGB stars of metallicity $Z \geqslant 4 \times 10^{-3}$. The O–Al trend of M107 is shown in the right panel of Figure 4.

The O abundances measured in M107 stars span a range of ∼0.4 dex, significantly smaller than observed in the GC discussed so far. While the small number of M107 stars with measured O abundances might partly account for this difference, it is, however, hard to believe that stars with O abundances below [O/Fe] $= -0.1$ can be detected. Such a small spread is motivated by the relative high metallicity of M107 because O burning becomes less and less efficient as the metallicity increases. This can be seen in the right panel of Figure 1, where we note that the line corresponding to $Z = 4 \times 10^{-3}$ never drops below δ[O/Fe] $= -0.3$.

The Al abundances do not help in this case. Despite the models predicting some Al production (δ[Al/Fe] $\sim +0.5$), no significant spread is observed because the FG stars in this cluster, those on the right side of the O–Al plane, with [O/Fe] ∼ 0.4–0.5, formed with a higher Al ([Al/Fe] $= +0.5$), compared to a purely solar scaled mixture; in this case, for the

same increase in the overall Al, no significant percentage increase of the surface Al is expected, in agreement with the observations.

4. CONCLUSIONS

We discuss the AGB scenario for the formation of multiple populations in GC, based on recent results from the APOGEE survey. This investigation is focused mainly on the interpretation of the Mg–Al anticorrelation, which compared to the largely used O–Na trend offers a much better tool to identify the potential polluters of the intra-cluster medium. This is due to the much higher sensitivity of Mg–Al cycling to temperature and metallicity. Furthermore, the interpretation of the Mg and Al content of giant stars is straightforward, since both species are not expected to undergo any alteration during the RGB evolution, even in the case of strong extra-mixing events.

To fully exploit the possibilities offered by the APOGEE observations, we examine five clusters, spanning the metallicity range $-2.3 < [Fe/H] < -1.0$. This is the first time that a self-enrichment scenario is tested against the O–Mg–Al data in a large sample of GC stars spanning such a wide (a factor ∼20) metallicity range.

The comparison between the data and the chemical composition of the ejecta of massive ($M \geqslant 4\,M_{\odot}$) AGB stars shows a remarkably good agreement. The observed O–Mg–Al spreads are reproduced and more importantly, the AGB yields follow the same trend with metallicity outlined by the observations, derived by comparing results of clusters with different metal content. In all the GC examined, dilution of AGB gas with pristine matter is required to match the observations. Part of SG stars in M92 and M13 appear to have formed from pure AGB ejecta, with no dilution.

The present analysis provides a strong indication that the nucleosynthesis experienced by AGB stars is characterized by the large variety of temperatures, changing according to the mass and the metallicity, required to reproduce the chemical patterns traced by GC stars.

P.V. acknowledges financial support from the Spanish Ministry of Economy and Competitiveness (MINECO) under the 2015 Severo Ochoa Program MINECO SEV-2015-0548. D.A.G.H. was funded by the RYC-2013-14182 fellowship and D.A.G.H. and O.Z. acknowledge support provided by the MINECO grant AYA-2014-58082-P. S.M. has been supported by the Premium Postdoctoral Research Program of the Hungarian Academy of Sciences, and by the Hungarian NKFI grants K-119517 of the Hungarian National Research, Development and Innovation Office. Funding for SDSS-III has been provided by the Alfred P. Sloan Foundation, the Participating Institutions, the National Science Foundation, and the U.S. Department of Energy Office of Science. The SDSS-III website is http://www.sdss3.org/. SDSS-III is managed by the Astrophysical Research Consortium for the Participating Institutions of the SDSS-III Collaboration including the University of Arizona, the Brazilian Participation Group, Brookhaven National Laboratory, University of Cambridge, Carnegie Mellon University, University of Florida, the French Participation Group, the German Participation Group, Harvard University, the Instituto de Astrofsica de Canarias, the Michigan State Notre Dame JINA Participation Group, Johns Hopkins University, Lawrence Berkeley National Laboratory, Max Planck Institute for Astrophysics, New Mexico State University, New York University, Ohio State University, Pennsylvania State University, University of Portsmouth, Princeton University, the Spanish Participation Group, University of Tokyo, University of Utah, Vanderbilt University, University of Virginia, University of Washington, and Yale University.

Facility: SDSS-III(APOGEE).

Software: ATON.

REFERENCES

Bastian, N., Lamers, H. J. G. L. M., de Mink, S. E., et al. 2013, MNRAS, 436, 2398
Blöcker, T., & Schönberner, D. 1991, A&A, 244, L43
Bloecker, T. 1995, A&A, 297, 727
Carretta, E., Bragaglia, A., Gratton, R. G., et al. 2009, A&A, 505, 117
Carretta, E., Gratton, R. G., Bragaglia, A., D'Orazi, V., & Lucatello, S. 2013, A&A, 550, A34
D'Antona, F., Vesperini, E., D'Ercole, A., et al. 2016, MNRAS, 458, 2122
Decressin, T., Meynet, G., Charbonnel, C., Prantzos, N., & Ekström, S. 2007, A&A, 464, 1029
D'Ercole, A., Vesperini, E., D'Antona, F., McMillan, S. L. W., & Recchi, S. 2008, MNRAS, 391, 825
de Mink, S. E., Pols, O. R., Langer, N., & Izzard, R. G. 2009, A&A, 507, L1
Denisenkov, P. A., & Denisenkova, S. N. 1990, SvAL, 16, 275
Denissenkov, P., & Hartwick, F. D. A. 2014, MNRAS, 437, L21
García-Hernández, D. A., Mészáros, S., Monelli, M., et al. 2015, ApJL, 815, L4
Gratton, R. G., Carretta, E., & Bragaglia, A. 2012, A&ARv, 20, 50
Majewski, S. R., Schiavon, R. P., Allende Prieto, C., et al. 2016, AJ, submitted (arXiv:1509.05420)
Mészáros, S., Martell, S. L., Shetrone, M., et al. 2015, AJ, 149, 153
Piotto, G., Bedin, L. R., Anderson, J., et al. 2007, ApJL, 661, L53
Renzini, A. 2008, MNRAS, 391, 354
Renzini, A., D'Antona, F., Cassisi, S., et al. 2015, MNRAS, 454, 4197
Ventura, P., Carini, R., & D'Antona, F. 2011, MNRAS, 415, 3865
Ventura, P., & D'Antona, F. 2011, MNRAS, 410, 2760
Ventura, P., D'Antona, F., Mazzitelli, I., & Gratton, R. 2001, ApJL, 550, L65
Ventura, P., Di Criscienzo, M., Carini, R., & D'Antona, F. 2013, MNRAS, 431, 3642
Ventura, P., Di Criscienzo, M., D'Antona, F., et al. 2014, MNRAS, 437, 3274